Available online at www.sciencedirect.com
ScienceDirect
Journal of Solid State Chemistry 180 (2007) 3247–3252
JOURNAL OF SOLID STATE CHEMISTRY
www.elsevier.com/locate/jssc

Water-containing derivative phases of the $Sr_{n+1}Fe_nO_{3n+1}$ series

M. Lehtimäki[a,b], A. Hirasa[a], M. Matvejeff[a,b], H. Yamauchi[a], M. Karppinen[a,b,*]

[a]*Materials and Structures Laboratory, Tokyo Institute of Technology, Yokohama 226-8503, Japan*
[b]*Laboratory of Inorganic and Analytical Chemistry, Helsinki University of Technology, P.O. Box 6100, FI-02015 TKK, Finland*

Received 29 June 2007; received in revised form 17 September 2007; accepted 18 September 2007
Available online 26 September 2007

Abstract

The $n = 1$, 2, 3 and ∞ members of the homologous series $Sr_{n+1}Fe_nO_{3n+1}$ of layered iron oxides are investigated for their tendency to accept additional layers of water in their crystals. The phases possess a Ruddlesden–Popper-type SrO-$(SrO\text{-}FeO_2)_n$ crystal structure, where the $n = \infty$ limit is nothing but the perovskite structure. It is revealed that the $n = 1$, 2 and 3 phases readily accommodate one or two layers of water between adjacent SrO layers, whereas the $n = \infty$ member which lacks the SrO–SrO double-layer unit remains intact in the presence of water. The speed of the water intercalation process is found to decrease with increasing n. Among the layered water derivatives, the $n = 2$ phase with two water molecules per formula unit, i.e. $Sr_3Fe_2O_7 \cdot 2H_2O$, was found to be most stable.
© 2007 Elsevier Inc. All rights reserved.

Keywords: Iron oxides; Ruddlesden–Popper structure; Homologous series; Water intercalation

1. Introduction

Multilayered transition metal oxides have been in the focus of research efforts for the last two decades due to their ability to exhibit a wide variety of interesting functional properties, such as high-T_c superconductivity, oxide-ion conductivity, and high-performance magnetoresistance and thermoelectric characteristics. For researchers working in the field, discovering the limits for each new family of materials by searching for the simplest and also the most complex members of it is of the very scientific interest. In addition, such new-material search contributes to extending the frontier of material candidates for the next-generation advanced applications. As a toolbox for the practical new-material hunt, the concepts of "homologous series" [1] and "layer-engineering" [2–4] have proven to be useful. The high-T_c superconductor family serves as an impressive example: the huge variety of the presently known phases are—in a universal manner—categorized as members of different homologous series, which then in turn serve as a platform for the next-stage design of new materials realized by simply inserting/removing atomic layers in/from the existing phases.

An exciting means of layer-engineering, i.e. topotactic water intercalation, was recognized recently as it was found that some of the layered oxides are prone to accommodate additional water layers in their crystal structures upon being exposed to ambient air (even at room temperature). Examples of the frontier materials discovered through water-intercalation processes include the watery superconductors of $Ba_2Ca_{n-1}Cu_nO_{2n+2} \cdot yH_2O$ [5] and $Na_xCoO_2 \cdot yH_2O$ [6]. Upon water intercalation the unit cell of the parent oxide phase is elongated along the layer-piling (c-axis) direction, whereas the originally existing layers are affected only a little.

The parent phases of the $Ba_2Ca_{n-1}Cu_nO_{2n+2} \cdot yH_2O$ watery superconductors form a homologous series of $Ba_2Ca_{n-1}Cu_nO_{2n+2}$ of Ruddlesden–Popper (RP) type [7,8] crystal structures. In addition to the $Ba_2Ca_{n-1}Cu_nO_{2n+2}$ series several other RP phases with a general formula of $A_{n+1}B_nO_{3n+1}$ and a layer sequence of AO–AO–BO_2–$(AO$–$BO_2)_{n-1}$ have been found to react with water to form well-defined water-derivative phases, namely Ba_2ZrO_4 ($n = 1$) [9], $(H,Na,Eu,La)_2TiO_4$ ($n = 1$) [10,11], $KLnTiO_4$ (Ln = lanthanoid) ($n = 1$) [12], $NaLaNb_2O_7$ ($n = 2$) [13],

*Corresponding author. Laboratory of Inorganic and Analytical Chemistry, Helsinki University of Technology, P.O. Box 6100, FI-02015 TKK, Finland. Fax: +359 9 462 373.
E-mail address: maarit.karppinen@tkk.fi (M. Karppinen).

0022-4596/$ - see front matter © 2007 Elsevier Inc. All rights reserved.
doi:10.1016/j.jssc.2007.09.020

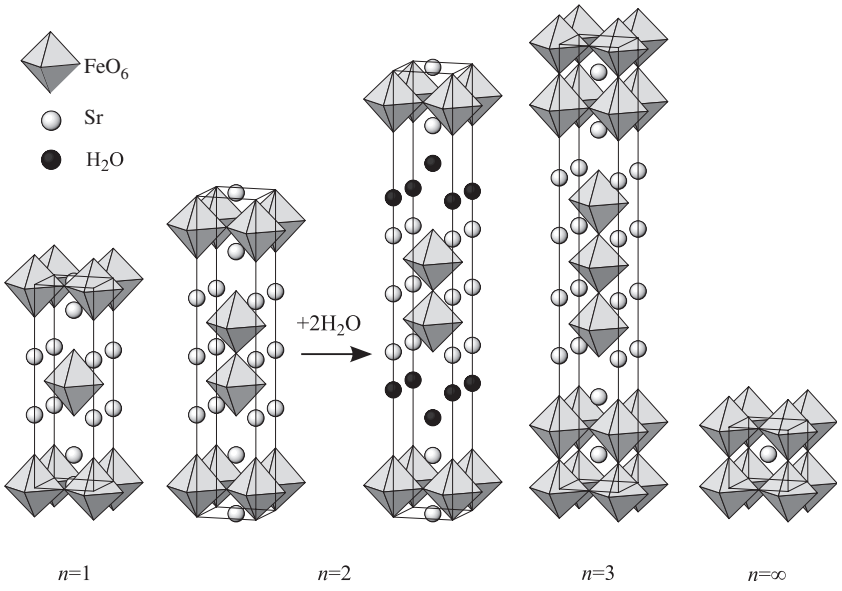

Fig. 1. Crystal structures of the of $Sr_{n+1}Fe_nO_{3n+1}$ phases with $n = 1$, 2, 3 and ∞ [23,24], and the water derivative of the $n = 2$ phase, $Sr_3Fe_2O_7 \cdot 2H_2O$ [22].

Ba_3InBiO_7 ($n = 2$) [14], $K_2SrTa_2O_7$ ($n = 2$) [15], $(Na,K)_2(Ca,Sr,La)_2Ta_3O_{10}$ ($n = 3$) [16,17], $Sr_3LnFe_3O_{10}$ ($n = 3$) [18,19], and $Sr_{n+1}Co_nO_{3n+1}$ ($n = 2$, 3) [20,21]. In these compounds, commonly intercalated are 1–2 water molecules per formula unit.

Recently we reported a novel water-derivative phase for the RP iron oxide, $Sr_3Fe_2O_7$ [22]. In the present contribution the work is extended to cover three other members of the $Sr_{n+1}Fe_nO_{3n+1}$ homologous series. Fig. 1 schematically shows the crystal structures of all the four members, $n = 1$, 2, 3 and ∞, of the $Sr_{n+1}Fe_nO_{3n+1}$ series investigated in the present work plus the water derivative of the $n = 2$ phase. Note that the $n = \infty$ member is nothing but the $SrFeO_3$ perovskite.

2. Sample syntheses

Samples of $Sr_{n+1}Fe_nO_{3n+1}$ with $n = 1$, 2, 3 and ∞ were synthesized from stoichiometric amounts of Sr and Fe precursors, starting with a combination of either $SrCO_3$ and Fe_2O_3 ($n = 1$, 3, ∞) or $Sr(NO_3)_2$ and $Fe(NO_3)_3 \cdot 9H_2O$ ($n = 2$). For each case the synthesis conditions employed were carefully optimized on the basis of thermal stability of the phase concerned. The $n = 2$ and ∞ members of the series are stable at high temperatures (above 1000 °C), whereas the $n = 1$ and 3 members are stable only at low temperatures and therefore rather difficult to be obtained in single-phase form [23–25].

The Sr_2FeO_4 ($n = 1$) sample was synthesized through a nitrate precipitation route, by dissolving the starting materials in concentrated nitric acid and then letting the excess solvent evaporate on a hot plate, after which the nitrate residue thus obtained was calcined in air at 600 °C for 12 h. The final heat treatment was carried out in O_2 gas flow at 750 °C for ca. 70 h. The $Sr_3Fe_2O_7$ ($n = 2$) sample was synthesized through another wet-chemical route, in which the metal cations are chelated by ethylenediaminetetraacetic acid (EDTA) from an aqueous nitrate solution [22]. The excess solution was evaporated in a hot water bath and the resultant dry gel was calcined in air at 450 °C for 4 h. The final heat treatment was carried out in air at 1000 °C with several intermediate grindings for ca. 110 h in total. The $Sr_4Fe_3O_{10}$ ($n = 3$) and $SrFeO_3$ ($n = \infty$) members were obtained through solid-state synthesis routes. The well-ground precursor mixtures were heat treated in air at 850 °C (for ca. 70 h) and 1100 °C (for 24 h), respectively. For all the four phases, the sample was quenched to room temperature after the final heat treatment, followed by immediate characterization of the as-synthesized sample for phase purity and lattice parameters by means of X-ray powder diffraction (XRD; Rikagu RINT2000 equipped with a rotating Cu anode). After the characterization, the as-synthesized samples were exposed to ambient air (temperature 20 ± 2 °C, relative humidity $45 \pm 10\%$) or dipped in distilled water in order to study their tendencies to form water derivatives.

3. Results and discussion

X-ray diffraction patterns for the as-synthesized samples of the parent $Sr_{n+1}Fe_nO_{3n+1}$ phases are shown in Fig. 2. It is seen that the $n = 2$, 3 and ∞ members were obtained in XRD-pure forms, but in the pattern for the $n = 1$ sample peaks due to $SrCO_3$ are detected besides those for the target phase. It should be noted that in the case of the $n = 3$ phase it was hard to completely eliminate the possibility of partial substitution of Fe with CO_3 (cf. $Sr_4Fe_{2.6}(CO_3)_{0.4}O_{10}$ reported in Ref. [26]). However, no sign of any impurity

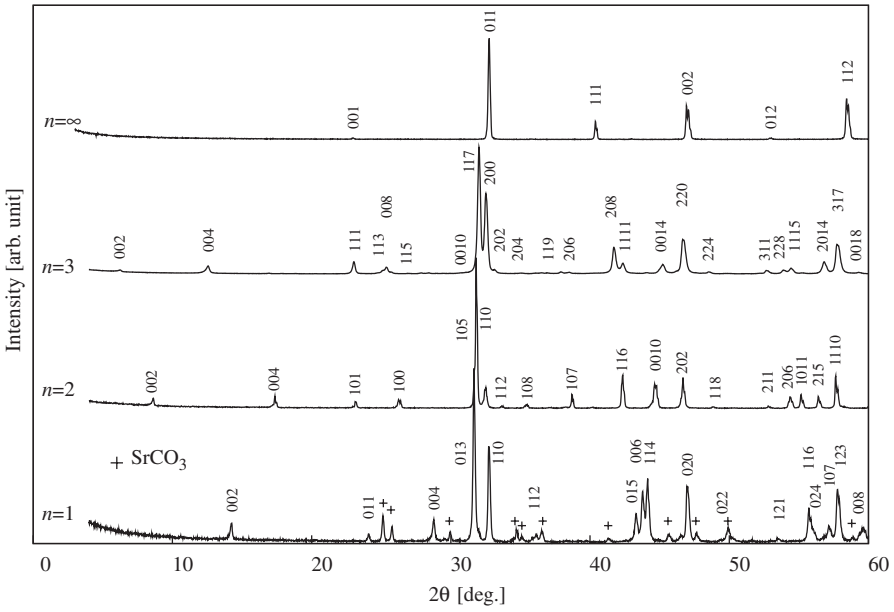

Fig. 2. XRD patterns for the as-synthesized samples of $Sr_{n+1}Fe_nO_{3n+1}$ with $n = 1$, 2, 3 and ∞. The patterns are indexed in tetragonal space group I_4/mmm for $n = 1$, 2 and 3 and cubic space group $Pm-3m$ for $n = \infty$ (see the text).

phase was observed in the XRD pattern in which the excess iron released due to the unwanted CO_3-for-Fe substitution would be residing. The lattice parameters of the parent phases were determined (in space group I_4/mmm for $n = 1$, 2 and 3 and $Pm-3m$ for $n = \infty$) as follows: parameter a at ~3.86(2) Å for all the four phases and parameter c at 12.4(1), 20.2(1) and 28.1(1) Å for $n = 1$, 2, and 3, respectively. Note that for $SrFeO_3$ the cubic space group $Pm-3m$ was assumed for the sake of better comparison to the RP phases, even though in practice the XRD pattern reveals a small tetragonal/orthorhombic splitting (apparently due to oxygen deficiency).

As previously reported [22], the $n = 2$ member, $Sr_3Fe_2O_7$, readily absorbs water to form a derivative phase when exposed to ambient air. The formation of the water derivative (with two water molecules per formula unit) was evidenced by monitoring the appearance and growth of its low-angle (0 0 2) diffraction peak at $2\theta = 6.2^\circ$ (coinciding with the disappearance of the (0 0 2) reflection of the parent RP phase at 8.6°), see Fig. 3. The lattice parameters of the watery derivative phase were refined from the XRD data in space group I_4/mmm as follows: $a = 3.89(2)$ Å and $c = 28.1(1)$ Å. Comparison to those for the parent RP phase reveals that the c parameter expands by ~4.0 Å [$= 0.5(28.1-20.2)$ Å] per formula unit. This value of c-parameter expansion is highly comparable to those previously reported for the water derivatives of the $Sr_3LnFe_3O_{10}$ phases [18,19]. In Ref. [22] also shown was that the speed of the derivative-phase formation depends on the exact oxygen content of the parent RP phase, increasing with decreasing oxygen content. However, even for the most reduced sample of the parent RP phase it took several days to complete the derivative-phase formation. Here it should be noted that upon extreme water exposure

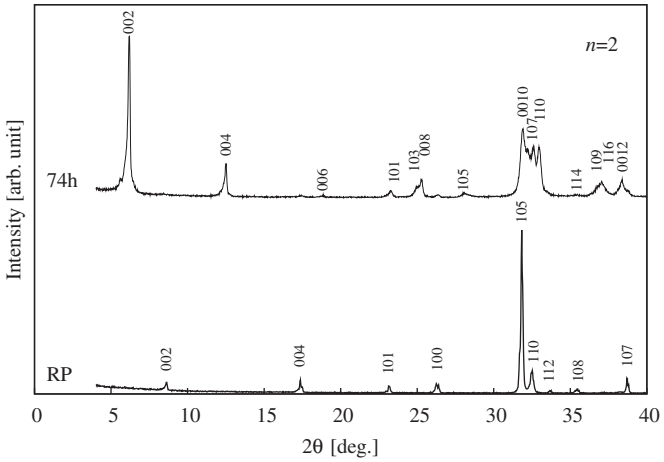

Fig. 3. XRD patterns for a $Sr_3Fe_2O_7$ sample ($n = 2$) recorded immediately after the synthesis (the bottom pattern) and after a 74-h exposure to ambient air (the upper pattern). Indices are for the $Sr_3Fe_2O_7$ (I_4/mmm) and the $Sr_3Fe_2O_7 \cdot 2H_2O$ (I_4/mmm) structure, respectively.

(achieved by keeping the specimen in saturated humidity or dipping it in distilled water) the derivative phase was found to transform to the phase, $Sr_3Fe_2(OH)_{12}$, of a cubic crystal structure [22,27]. On the other hand, upon heating the layered water-derivative phase was found to release the intercalated water in two distinct steps, one about 70 °C and another about 200 °C, according to the TG data measured for the phase [22]. Apparently the first water-loss step corresponds to the formation of an intermediate water-derivative phase with one water molecule per formula unit [18,19,22].

Also the $n = 1$ member, Sr_2FeO_4, was found to absorb water to form a layered watery derivative. As for the rate of

the derivative-phase formation, the water molecules seem to enter the $n=1$ phase much faster than the $n=2$ phase. At the same time the layered water derivative of the $n=1$ phase was found to be more unstable than that of the $n=2$ phase, rapidly decomposing to $Sr(OH)_2 \cdot H_2O$ and $Sr_3Fe_2(OH)_{12}$. Therefore it was practically impossible to isolate the derivative phase in single-phase form. In Fig. 4, shown are XRD patterns for an $n=1$ sample recorded immediately after the synthesis and after a 1-h exposure to open air. In the latter pattern, peaks due to the parent RP phase are still visible together with those for the derivative phase (and the initial $SrCO_3$ impurity) and $Sr(OH)_2 \cdot H_2O$, while those for the $Sr_3Fe_2(OH)_{12}$ phase are not yet seen. From the position of the (0 0 4) peak at $2\theta = 16.4^\circ$ (assuming space group I_4/mmm), the c parameter of the

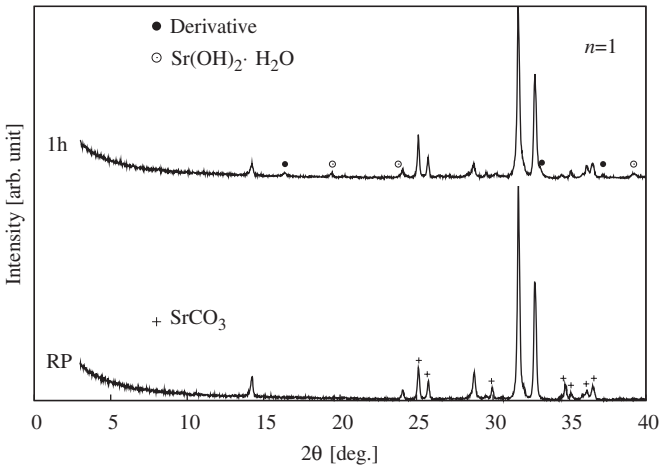

Fig. 4. XRD patterns for a Sr_2FeO_4 sample ($n=1$) recorded immediately after the synthesis (the bottom pattern) and after a 1-h exposure to ambient air (the upper pattern).

derivative phase was estimated at ~21.6 Å. Accordingly the expansion of the lattice along the c-axis direction upon the water-derivative formation was calculated at ~4.6 Å per formula unit.

Like the lower members of the $Sr_{n+1}Fe_nO_{3n+1}$ series, the $n=3$ member was also found to absorb water to form water-derivative phase(s); see Fig. 5 for the XRD patterns recorded for an $n=3$ sample after different periods of air exposure. However, compared with the cases of the $n=1$ and 2 members, the water intercalation process is considerably slower: even the samples kept in open air for several weeks contained traces of the original RP phase. It also seems that the water intercalation produces not a single water derivative phase but a mixture of various derivatives with different water contents, making the identification of the diffraction peaks appearing upon the water intercalation somewhat uncertain. Also seen from Fig. 5 is that the water derivative(s) are not completely stable but decompose finally to $Sr(OH)_2 \cdot 8H_2O$ (and $Sr_3Fe_2(OH)_{12}$).

In Fig. 6 shown are TG curves for the fully hydrated samples of $n=2$ and 3 (containing the maximum amounts of the corresponding layered water derivatives) measured in O_2 gas flow with a heating rate of 2 °C/min. For both the systems, the intercalated water is lost in two or more steps. Moreover seen is that in both cases the dehydration is completed (and the RP phase is recovered after the last water molecule has been removed) at ~230 °C. However, the low-temperature behavior is different for the two systems: for $n=3$ some of the water molecules are removed without any clear activation energy right above room temperature, whereas for $n=2$ a clear onset of water loss is seen at ~70 °C. This is consistent with our observation that in open air at room temperature a mixture

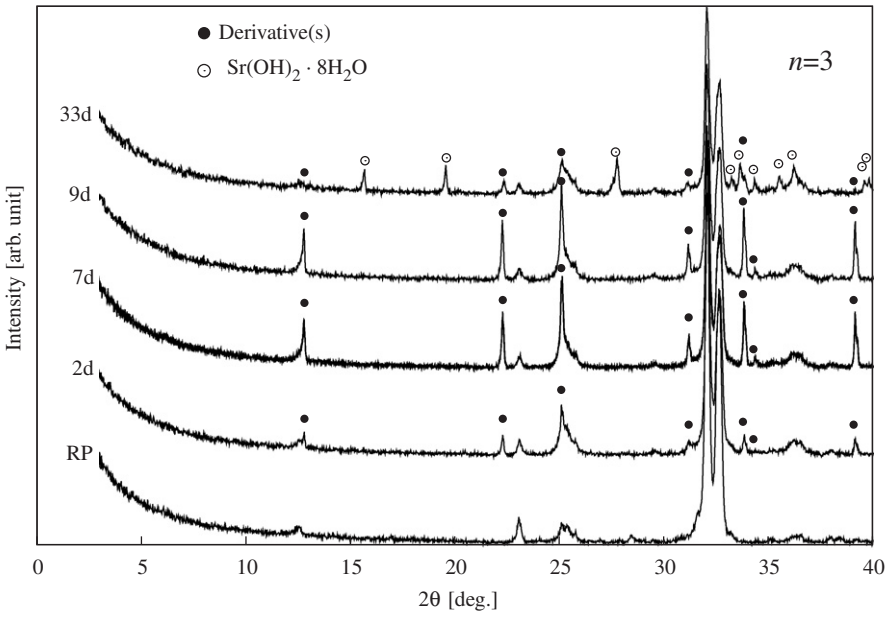

Fig. 5. XRD patterns for a $Sr_4Fe_3O_{10}$ sample ($n=3$) recorded immediately after the synthesis (the bottom pattern) and an air-exposure of different lengths (ranging from 2 to 33 days for the uppermost pattern).

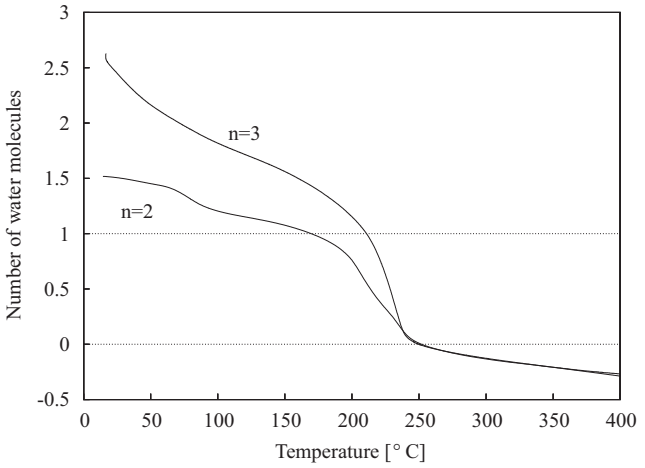

Fig. 6. TG curves recorded for the layered water derivatives of $Sr_3Fe_2O_7$ (after an air-exposure of ~3 days) and $Sr_4Fe_3O_{10}$ (after an air-eposure of ~10 days) in O_2 gas flow with a heating rate of 2 °C/min. The weight losses below ~70 °C apparently mark the evaporation of adsorbed water, whereas the higher-temperature weight losses are believed to be due to the deintercalation of absorbed water molecules.

of two (or more) water-derivative phases is obtained for $n = 3$, whereas for $n = 2$ the hydration process rapidly ends up with the formation of the relatively stable derivative phase with two water molecules per formula unit.

Contrary to the $n = 1$, 2 and 3 members, the end member of the $Sr_{n+1}Fe_nO_{3n+1}$ series, i.e. the $SrFeO_3$ perovskite with $n = \infty$, was found not to absorb water. Since the oxygen content of the parent phase may affect the speed of the water intercalation process [22], the as-air-synthesized $SrFeO_3$ sample (with the actual oxygen content determined at 2.8 with cerimetric titration) was oxygen-reduced by means of various post-annealing treatments to different oxygen contents ranging from 2.5 to 2.8. However, none of the oxygen-controlled $n = \infty$ samples showed any reactivity towards water-derivative formation, as all the samples remained completely stable even when dipped in water. Hence we conclude that only the $Sr_{n+1}Fe_nO_{3n+1}$ phases that possess the $(SrO)_2$ double layer, not found in the structure of the $n = \infty$ member of the series, are able to welcome additional layers of water.

4. Conclusion

Layered iron oxides of the Ruddlesden–Popper series, $Sr_{n+1}Fe_nO_{3n+1}$, were systematically investigated for their tendencies to be hydrated by means of topotactic intercalation of additional water molecule layers. It was revealed that the $n = 1$, 2 and 3 phases with a SrO-$(SrO\text{-}FeO_2)_n$ layer sequence readily accommodate one or two water layers into the SrO–SrO double-layer block, whereas the $n = \infty$ member which lacks such a double-layer unit remains intact against water. Moreover, for the $n = 1$, 2 and 3 phases a trend was seen that the water intercalation process became more sluggish with increasing n.

Among the layered water derivatives formed, the $n = 2$ phase with two water molecules per formula unit, i.e. $Sr_3Fe_2O_7 \cdot 2H_2O$, was found to be most stable. However, after all, all the layered water derivatives regardless of the n value were found to decompose to either simple binary oxides and hydroxides or $(Sr_3Fe_2(OH)_{12}$ upon elongated exposure to humid air and/or dipping in water.

Acknowledgments

This work was supported by the Academy of Finland (Decision no. 110433) and also MSL's International Collaborative Research Project-2005 (Tokyo Tech). One of us (M.M.) acknowledges Finnish Cultural Foundation and Scandinavia-Japan Sasakawa Foundation for their financial support.

References

[1] H. Yamauchi, M. Karppinen, S. Tanaka, Physica C 263 (1996) 146; M. Karppinen, H. Yamauchi, Mater. Sci. Eng. R 26 (1999) 51.
[2] B. Raveau, M. Hervieu, D. Pelloquin, C. Michel, R. Retoux, Z. Anorg. Allg. Chem. 631 (2005) 1831.
[3] H. Yamauchi, K. Sakai, T. Nagai, Y. Matsui, M. Karppinen, Chem. Mater. 18 (2006) 155.
[4] I. Grigoraviciute, H. Yamauchi, M. Karppinen, J. Am. Chem. Soc. 129 (2007) 2593.
[5] T. Hosomi, H. Suematsu, H. Fjellvåg, M. Karppinen, H. Yamauchi, J. Mater. Chem. 9 (1999) 1141;
H. Yamauchi, M. Karppinen, T. Hosomi, H. Fjellvåg, Physica C 338 (2000) 38;
M. Karppinen, T. Hosomi, H. Yamauchi, Physica C 382 (2002) 276.
[6] K. Takada, H. Sakurai, E. Takayama-Muromachi, F. Izumi, R.A. Dilanian, T. Sasaki, Nature 422 (2003) 53.
[7] S.N. Ruddlesden, P. Popper, Acta Crystallogr., Sect. A 10 (1957) 538, 11 (1958) 54.
[8] $Ba_2Ca_{n-1}Cu_nO_{2n+2}$ phases are A-cation ordered, oxygen-deficient RP phases of $A_{n+1}B_nO_{3n+1}$.
[9] R.V. Shpanchenko, E.V. Antipov, L.M. Kovba, Mater. Sci. Forum 133–136 (1993) 639.
[10] K. Toda, Y. Kameo, S. Kurita, M. Sato, Bull. Chem. Soc. Jpn. 69 (1996) 349.
[11] S. Nishimoto, M. Matsuda, M. Miyake, J. Solid State Chem. 178 (2005) 811.
[12] R.E. Schaak, T.E. Mallouk, J. Solid State Chem. 161 (2001) 225.
[13] M. Sato, J. Abo, T. Jin, Solid State Ionics 57 (1992) 285.
[14] A. Baszczuk, J. All. Comp. 414 (2006) 287.
[15] T. Kodenkandath, J.B. Wiley, Mater. Res. Bull. 35 (2000) 1737.
[16] K. Toda, T. Teranishi, M. Takahashi, Z.-G. Ye, M. Sato, Solid State Ionics 113–115 (1998) 501.
[17] R.E. Schaak, T.E. Mallouk, J. Solid State Chem. 155 (2000) 46.
[18] T. Nishi, K. Toda, F. Kanamaru, T. Sakai, Key Eng. Mater. 169–170 (1999) 235.
[19] D. Pelloquin, J. Hadermann, M. Giot, V. Caignaert, C. Michel, M. Hervieu, B. Raveau, Chem. Mater. 16 (2004) 1715.
[20] D. Pelloquin, N. Barrier, A. Maignan, V. Caignaert, Solid State Sci. 7 (2005) 853.
[21] D. Pelloquin, N. Barrier, D. Flahaut, V. Caignaert, A. Maignan, Chem. Mater. 17 (2005) 773.
[22] M. Matvejeff, M. Lehtimäki, A. Hirasa, Y.H. Huang, H. Yamauchi, M. Karppinen, Chem. Mater. 17 (2005) 2775.
[23] C. Brisi, P. Rolando, Ann. Chim. (Rome) 59 (1969) 385.
[24] S.E. Dann, M.T. Weller, D.B. Currie, J. Solid State Chem. 92 (1991) 237; S.E. Dann, M.T. Weller, D.B. Currie, J. Solid State Chem. 97 (1992) 179;

S.E. Dann, M.T. Weller, D.B. Currie, M.F. Thomas, A.D. Al-Rawwas, J. Mater. Chem. 3 (1993) 1231.
[25] A. Fossdal, M.-A. Einarsrud, T. Grande, J. Solid State Chem. 177 (2004) 2933.
[26] Y. Bréard, C. Michel, M. Hervieu, B. Raveau, J. Mater. Chem. 10 (2000) 1043.
[27] N.N. Nevskii, B.N. Ivanov-Emin, N.A. Nevskaya, G.Z. Kaziev, N.V. Belov, Dokl. Akad. Nauk SSSR 264 (1982) 857.